

Hiroaki Nagai · Koji Murata · Takato Nakano

Defect detection in lumber including knots using bending deflection curve: comparison between experimental analysis and finite element modeling

Received: May 28, 2008 / Accepted: December 4, 2008 / Published online: February 20, 2009

Abstract A new method has been developed for detecting localized defects such as edge knots using a bending deflection curve. The coordinates of a bottom edge (edgeline) of an unloaded piece of lumber are extracted from a digital image, and a bending deflection curve is obtained from the displacement of the edgeline of the lumber using a digital image correlation (DIC) technique. Depending on the knots within the beam, the bending deflection curve is shifted from the curve of a defect-free beam. The measured bending deflection curve is regressed to a theoretical curve by elementary beam theory. A finite element method (FEM) model of the beams including defects as simplified knot structure has been performed. Comparison between the bending experiment and FEM analysis shows that cross-sectional reductions cause characteristic variations in the bending deflection curves depending on the position of encased knots, and local grain distortions cause variations in the curves depending on the direction of spike knots. Using the residual variance between the measured deflection curve and a polynomial regression curve, it is possible to detect knots at which failures initiate.

Key words Bending deflection curve · Defect detection · Knot · Digital image correlation

Introduction

Lumbers usually contain defects such as knots and fiber deviations in the vicinity of knots. The presence of these defects strongly affects the strength and stiffness of lumbers.

Because knots are regarded as the major strength-reducing defects, studies to consider the effect of knots and the fiber deviations in the vicinity of knots on the strength of lumbers have been carried out by many researchers (e.g., Mitsuhashi et al.¹).

In past decades, a large number of studies have been performed in the field of nondestructive testing of wood. In these studies, many physical properties of lumbers have been used for the detection of knots. For example, the optical properties of a lumber surface such as color and gloss have been employed.^{2,3} Furthermore, several automated visual inspection systems have been developed.^{4,5} However, optical information does not directly reflect the mechanical properties of the defects. Using X-rays or gamma rays, the density distribution in lumbers can be determined.^{6,7} Radiation techniques are based on the fact that knots have a higher density than the surrounding material. In research conducted by Boström,⁶ the size, location, and even the shape of knots were obtained. Thermographic measurements have also been employed for the detection of knots and the slope of grains in lumbers.⁸ Thermal methods are based on the differences in the thermal conductivity and the heat absorption of knots and the surrounding material. Among other methods employed for the detection of knots, an ultrasonic sound technique based on longitudinal stress wave speed⁹ and a microwave technique using a microwave scanner have been developed. In particular, microwave techniques are being seriously considered for machine grading systems.^{10,11} Although these methods have produced good results on a laboratory scale, it will be difficult to achieve cost efficiency if these methods are introduced in small mills in Japan.

To study the mechanical properties of a lumber effectively, its response to a mechanical stimulus has to be observed. The most widely applied machine grading principle is to measure the bending modulus of elasticity (MOE) of lumbers. If a lumber contains a serious defect, the bending deflection curve may deviate from the theoretical curve. Murata et al.¹² measured the strain distribution in the vicinity of a knot by a four-point bending test using a digital image correlation (DIC) technique. In the present study, a

H. Nagai (✉) · K. Murata · T. Nakano
Division of Forest and Biomaterials Science, Graduate School
of Agriculture, Kyoto University, Kitashirakawa Oiwake-cho,
Sakyo-ku, Kyoto 606-8502, Japan
Tel. +81-75-753-6236; Fax +81-75-753-6300
e-mail: nagai@h1sparc1.kais.kyoto-u.ac.jp

Part of this article was presented at the 57th Annual Meeting of the Japan Wood Research Society, Hiroshima, Japan, August 2007

bending deflection curve was measured using the DIC technique, which yielded the subpixel displacement of the points under consideration using a correlation function and interpolation among pixels. The purpose of this study was to detect the localized defects in lumber including knots, at which failures initiate, by using the bending deflection curves.

Theory

When a wooden beam is loaded at the center of its span, its deflection y can be expressed by the elementary beam theory as follows:

$$y = -\frac{P}{48EI}(4x^3 - 3L^2x) = -\frac{P}{12EI}x^3 + \frac{PL^2}{16EI}x \quad (1)$$

where E is Young's modulus, I is the geometrical moment of inertia, L is the span length, P is the load at midspan, and x is the distance from the supporting point. In this study, Eq. 1 is regarded as a theoretical curve. The measured bending deflection coordinates are regressed to Eq. 2 at a given interval. Equation 2 is of the same form as Eq. 1.

$$y = \alpha x^3 + \beta x \quad (2)$$

If a regression region on the beam deflection curve includes a knot, the obtained curve changes characteristically. The change can be estimated in the following manner. First, it is expected that a knot breaks the local bending stiffness EI of the wooden beam. From Eqs. 1 and 2, EI can be calculated as follows:

$$EI_\alpha = -\frac{P}{12\alpha}, \quad EI_\beta = \frac{PL^2}{16\beta} \quad (3)$$

where EI_α and EI_β are obtained from the coefficients α or β in Eq. 2. Second, a knot distorts the grains in its vicinity, and the edge of the distorted region expands or shrinks along the direction of the beam height. To evaluate the deviation from the theoretical curve, a residual variance is obtained. The residual variance is the variance of the square sum of the difference between the measured deflection curve and the polynomial regression curve.

Experimental

Defect detection using static bending test

Twenty-one pieces of commercial 38×89 mm SPF lumber were used as specimens. The specimens were not identified with regard to species. Nondestructive three-point and destructive four-point bending tests were performed using a universal testing machine (Shimadzu; capacity, 98 kN) at a crosshead displacement speed of 5 mm min^{-1} .

The three-point bending test was carried out with a span length of 1400 mm. The maximum applied load was 1.5 kN, which was sufficiently smaller than the estimated rupture

load, because the modulus of rupture (MOR) for a clear spruce specimen was assumed to be 75 MPa.¹³

The bending deflection curve was calculated as follows, which was the same method as described in previous report.¹⁴ The deformation in the beam specimens was recorded by using two digital still cameras (Nikon D100; Zoomnikkor 105 mm) when a load of 1.5 kN was applied. The photographed region was on the left side of the specimen. The image size was 3008×2000 pixels. Each pixel was approximately equal to $0.15 \times 0.15 \text{ mm}^2$ (the dimensions of the observed field were approximately $450 \times 300 \text{ mm}^2$ for each camera). The coordinates of a bottom edge (edgeline) of an unloaded specimen were obtained from the digital image by using image processing techniques: Otsu binarization¹⁵ and edge detection techniques. The deformation at the edgeline was measured using in-house DIC software that yielded the subpixel displacement of the points under consideration using a correlation function and interpolation among the pixels. The deflection under a load of 0.2 kN was defined as the base deflection of the unloaded specimen to exclude the initial twist in the specimen during the measurements.

The measured bending deflection coordinates were regressed to Eq. 1 at the given interval (50 mm) and the coefficients were calculated using a polynomial regression. Because the interval affects the accuracy of defect detection, the sampling interval was experimentally determined in the previous analysis.

The destructive four-point bending test was performed with a loading span of 540 mm and a supporting span of 1620 mm at a crosshead displacement speed of 5 mm min^{-1} . The deformation in the beam specimen was recorded in the same manner as in the three-point bending test.

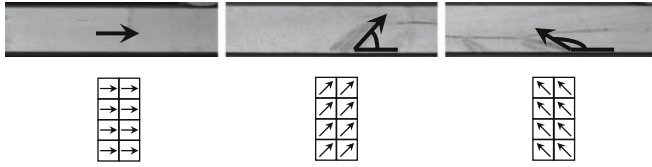
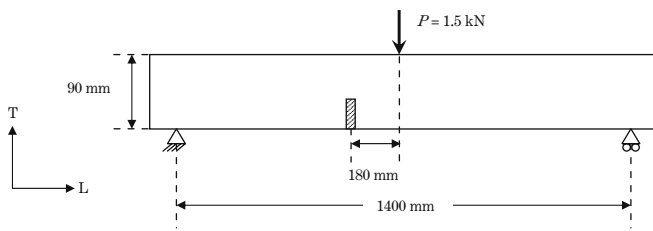
Study by finite element modeling (FEM) simulation

In the past few decades, studies concerning FE modeling of solid wood including knots have been performed by several wood research groups. For example, FE analyses based on linear fracture mechanics have been performed by a research group at Colorado State University.¹⁶⁻¹⁸ In these models, the flow-grain analogy¹⁹ was utilized to account for a localized grain deviation associated with knots. Another research group at Vienna University of Technology introduced a multisurface plasticity model for clear wood in consideration of elasto-plastic material²⁰ and this was applied to consider the effect of knots.²¹

In this study, however, a realistic knot structure is simplified to elucidate which properties of knots influence the bending deflection curves. Because encased knots break local flow-grain, a gap is used to represent encased knots. In the case of spike knots, they distort the grains in their vicinity. The regions of spike knots are only rotated on the axis of elements (material angle; MSC/NASTRAN) and use the same material properties as clear wood. The material angle is the local coordinate system of the elements and corresponds to the local grain distortions across knots. Figure 1 shows the rotation of the axis of the elements. In

Table 1. Specimen properties for finite element analysis

Specimen	Young's modulus		Shear modulus			Poisson ratio
	E_L (MPa)	E_T (MPa)	G_{LT} (MPa)	G_{LR} (MPa)	G_{RT} (MPa)	μ_{LT}
Clearwood (Sitka spruce)	10 700	430	618	500	43	0.51

**Fig. 1.** Rotation of axis of elements (material angle). Left, 0°; middle, 45°; right, 135°**Fig. 2.** Finite element method (FEM) model of the three-point bending test

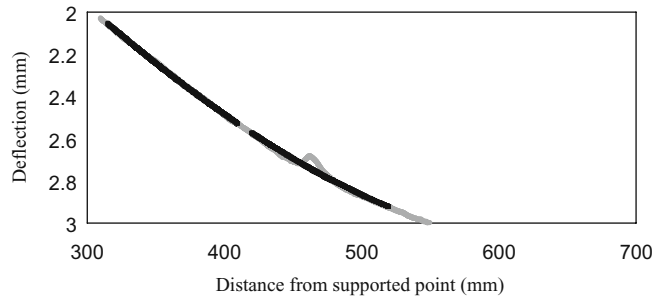
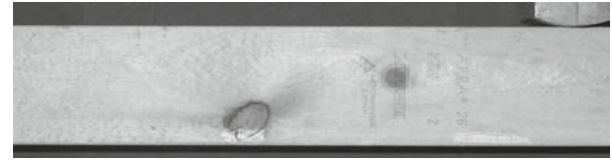
the regions with the spike knots, the grains in the vicinity of these knots ran from bottom left to top right (45°) or from bottom right to top left (135°).

A two-dimensional model of a wooden beam was simulated by using MSC/NASTRAN ver. 70.0 (Fig. 2). The beam was modeled with four node orthotropic linear elements and it was assumed that the elements deform as perfect elastic bodies. All the elements had a constant size of 0.625 (L) × 1.25 (T) mm, and the dimensions of the cross section of the beam model were 90 (T) × 40 (R) mm. Its span length was 1400 mm. The applied load to calculate bending deflection curves was 1.5 kN. The supporting point on one side was allowed to move along the x -axis (longitudinal direction) and was rotated freely around the z -axis (radial direction). The material properties of clear wood are listed in Table 1.

The defects were arrayed at a distance of 520 mm from the supporting point. The dimensions of the gap were 2.5 (L) × 20 (T) mm, and the dimensions of the region where the material angle was modified were 10 (L) × 20 (T) mm. The displacement of the nodes at the bottom edge was defined as the deflection curve. These bending deflection curves were analyzed by using the same method as that for digital imaging analysis, stated above.

Results and discussion

The bending deflection curves across the knots were found to be characteristically distorted according to the types

**Fig. 3.** Measured bending deflection curve (gray line) and polynomial regression curve (black line) for a beam with encased knots

of knots, for example, encased knots and spike knots. Figure 3 shows the measured bending deflection curve and the polynomial regression curves. The residual variance between the measured deflection curve and the polynomial regression curve in regions with knots was found to be higher than that for knot-free regions.

Figure 4 shows the EI profiles of the defect-free beams obtained from the coefficients of the polynomial regression curve at the given interval (50 mm). In the case of the defect-free beams, EI should have the same value. Deviation of the broken line near the origin appears to be caused by the effect of stress concentration at the supporting or loading point. In a comparison of EI profiles, EI_α enhances irregular factors. In order to avoid such effects, EI_β is used to identify the local bending stiffness EI in this study.

Figures 5 and 6 illustrate the profiles of EI and residual variance including the region with encased knots. Figure 5 shows a lumber including an encased knot that is located at the bottom edge (Type 1). The distance from the gap to the bottom edge is 0 mm in the FEM model (left side of Fig. 5). Figure 6 shows a lumber including an encased knot that is located near the bottom edge (Type 2). The distance from the gap to the bottom edge is 2.5 mm in the FEM model (left side of Fig. 6). Both the EI and residual variance profiles obtained from the experimental and FEM analyses exhibit similar patterns, as shown in Figs. 5 and 6. Comparison of the two profiles shows that the residual variance profile exhibits the characteristic pattern more clearly. The residual variance increases with the tangential length of the gap and a decrease in the distance from the edge of the specimen. It is concluded that the cross-sectional reductions

Fig. 4. Profiles of bending stiffness in defect-free beams, obtained from the coefficients EI_α (broken line) and EI_β (solid line) in Eq. 2. *Left*, FEM result; *right*, bending test ($P = 1.5$ kN)

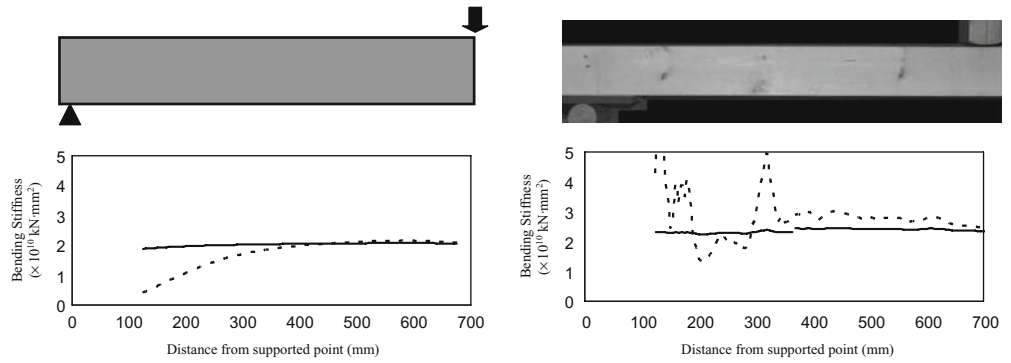


Fig. 5. Profiles of bending stiffness (broken line) and residual variance (solid line) from the FEM result (left) and from the bending test (right) (type 1 encased knot located at the edge of the lumber, $P = 1.5$ kN)

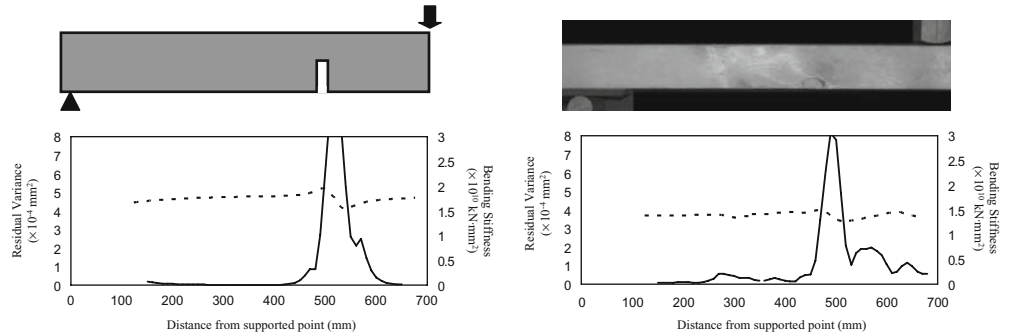


Fig. 6. Profiles of bending stiffness (broken line) and residual variance (solid line) from the FEM result (left) and from the bending test (right) (type 2 encased knot located near the edge of the lumber, $P = 1.5$ kN)

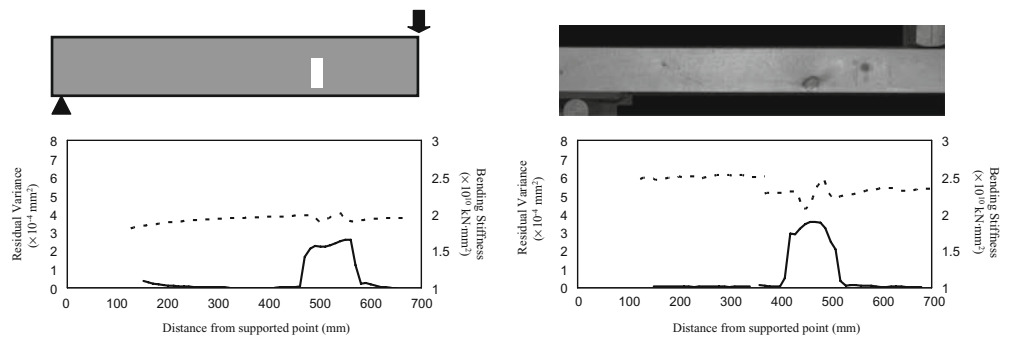
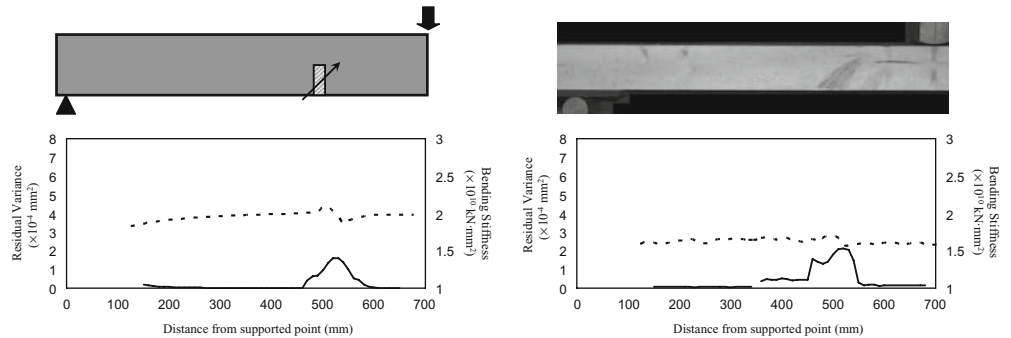


Fig. 7. Profiles of bending stiffness (broken line) and residual variance (solid line) from the FEM result (left) and from the bending test (right) (type 3 spike knot running from bottom left to top right, $P = 1.5$ kN)



cause the characteristic variations in the bending deflection curve observed at the encased knots.

The profiles of EI and residual variance including the region with spike knots are presented in Figs. 7 and 8. The material angles are 45° (Type 3) and 135° (Type 4) in Figs. 7 and 8, respectively. Elements with a material angle of 0° are regarded as defect-free materials. The experimental profiles display characteristic patterns similar to the FEM

profiles shown in Figs. 7 and 8. The profiles of the residual variance exhibit the characteristic pattern more clearly than those of EI . When other FEM models with different material angles (15° , 30° , 60° , 90° , etc.) were analyzed, it was found that the peak of the residual variance profile shows the maximum value for the material angles of 45° and 135° . The local grain distortion caused by spike knots influences the bending deflection curves. These results show that the

Fig. 8. Profiles of bending stiffness (*broken line*) and residual variance (*solid line*) from the FEM result (*left*) and from the bending test (*right*) (type 4 spike knot running from bottom right to top left, $P = 1.5$ kN)

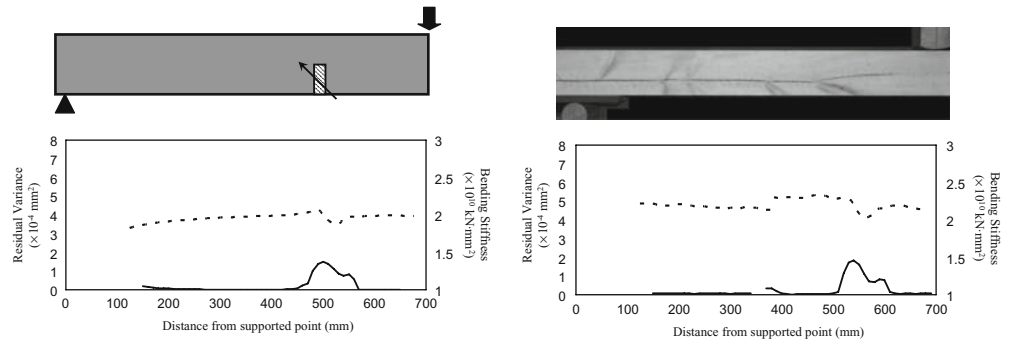
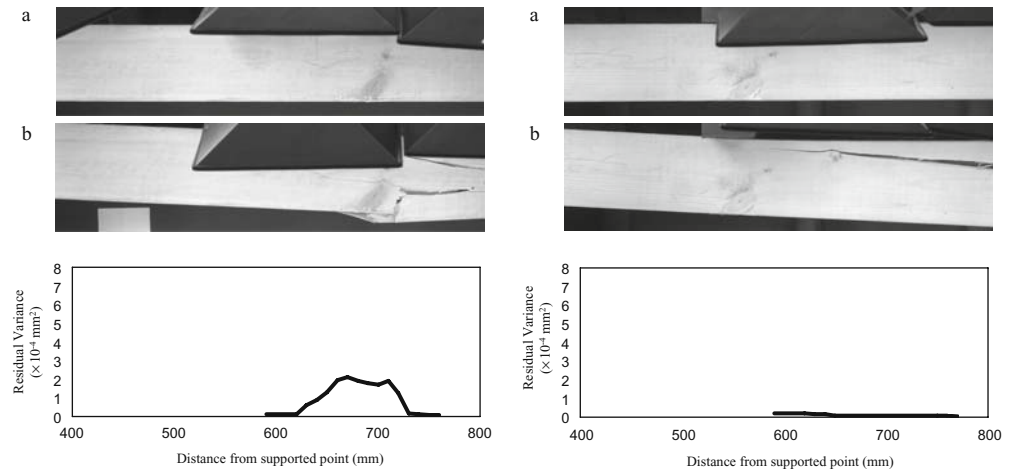


Fig. 9a, b. Failure images and profile of residual variance ($P = 1.5$ kN) **a** Lumber before testing, **b** lumber after failure. Specimens showing a clear peak in the residual variance profile around the knots (*left*) or not (*right*). Black object over the specimen is a lampshade



local grain distortion causes the characteristic variations in the bending deflection curve observed at the spike knots.

Images of typical failures that occurred during the destructive four-point bending test are illustrated in Fig. 9. The residual variance profile over the loading span obtained from the polynomial regression curve of Eq. 4 is also shown below the images.

$$y = -\frac{PL}{36EI} \left(3x^2 - 3Lx + \frac{L^2}{9} \right) \quad (4)$$

The specimens showing a clear peak in the residual variance profile around the knots always ruptured at the knots (left side of Fig. 9), while the specimens without a clear peak did not always rupture at the knots (right side of Fig. 9). Therefore, we believe that the method employing the residual variance profile of a bending deflection curve can be used to distinguish between the two types of knots in the same manner as visual grading.

Conclusions

Bending deflection curves across knots have been found to be characteristically distorted according to the types of knots. The residual variance between the measured deflection curve and the polynomial regression curve in regions with knots has been found to be higher than that of knot-free regions. Using a residual variance profile, it is possible

to detect knots at which failures initiate. Comparison between the bending experiment and FEM analysis showed that cross-sectional reductions cause the characteristic variations in the bending deflection curve depending on the position of the encased knots. Local grain distortions also cause variations in the curve depending on the direction of spike knots.

In this study, bending tests were combined with an image analysis technique. The bending deflection curves directly reflected the mechanical properties of defects. Therefore, this method used in combination with machine stress grading may give a better estimation of strength-reducing effects of localized defects.

References

- Mitsuhashi K, Poussa M, Puttonen J (2008) Method for predicting tension capacity of sawn timber considering slope of grain around knots. *J Wood Sci* 54:189–195
- Iwasaki S, Sadoh T (1991) Measurements of knots in hinoki and sugi lumbers by the optical scanning method (in Japanese). *Mokuzai Gakkaishi* 37:999–1003
- Sugimori M (1993) Recognition of longitudinal knot area by light reflection and image processing (in Japanese). *Mokuzai Gakkaishi* 39:1–6
- Pham DT, Alcock RJ (1998) Automated grading and defect detection: a review. *Forest Prod J* 48:34–42
- Estévez PA, Perez CA, Goles E (2003) Genetic input selection to a neural classifier for defect classification of radiata pine boards. *Forest Prod J* 53:87–94

6. Boström L (1999) State of the art on machine strength grading. Proceedings of the 1st RILEM Symposium on Timber Engineering, Stockholm, Sweden
7. Schajer GS (2001) Lumber strength grading using X-ray scanning. Forest Prod J 51:43–50
8. Sadoh T, Murata K (1993) Detection of knots in hinoki and karamatsu lumber by thermography (in Japanese). Mokuzai Gakkaishi 39:13–18
9. Karsulovic JT, León LA, Gaete L (2000) Ultrasonic detection of knots and annual ring orientation in *Pinus radiata* lumber. Wood Fiber Sci 32:278–286
10. Baradit E, Aedo R, Correa J (2006) Knot detection in wood using microwaves. Wood Sci Technol 40:118–123
11. Schajer GS, Orhan FB (2006) Measurement of wood grain angle, moisture content and density using microwaves. Holz Roh Werkst 64:483–490
12. Murata K, Masuda M, Ukyo S (2005) Analysis of strain distribution of wood using digital image correlation method – four-point bend test of timber including knots (in Japanese). Trans Visualiz Soc Jpn 25:57–63
13. Forest Products Laboratory (1999) Wood handbook: wood as an engineering material. General Technical Report FPL-GTR-113, United States Department of Agriculture, Forest Service, Madison, WI, pp 4–14
14. Nagai H, Murata K, Nakamura M (2007) Defect detection of lumber including knots using bending deflection curve (in Japanese). J Soc Mater Sci 56:326–331
15. Otsu N (1979) A threshold selection method from gray-level histograms. IEEE Trans Syst Man Cybern SMC-9:62–66
16. Cramer SM, Goodman JR (1983) Model for stress analysis and strength prediction of lumber. Wood Fiber Sci 15:338–349
17. Cramer SM, Goodman JR (1986) Failure modeling: a basis for strength prediction of lumber. Wood Fiber Sci 18:446–459
18. Zandbergs JG, Smith FW (1988) Finite element fracture prediction for wood with knots and cross grain. Wood Fiber Sci 20:97–106
19. Phillips GE, Bodig J, Goodman JR (1981) Flow-grain analogy. Wood Fiber Sci 14:55–64
20. Mackenzie-Helnwein P, Eberhardsteiner J, Mang HA (2003) A multi-surface plasticity model for clear wood and its application to the finite element analysis of structural details. Comput Mech 31:204–218
21. Fleischmann M, Krenn H, Eberhardsteiner J, Schickhofer G (2007) Experimental and numerical investigation of timber structures for the validation of an orthotropic plasticity model. Holz Roh Werkst 65:301–313